Applied Physics A (2018) 124:363
https://doi.org/10.1007/s00339-018-1782-3

Applied Physics A
Materials Science & Processing

Green synthesis of iron oxide nanoparticles by aqueous leaf extract of *Daphne mezereum* as a novel dye removing material

Nasrin Beheshtkhoo[1] · Mohammad Amin Jadidi Kouhbanani[1] · Amir Savardashtaki[2] · Ali Mohammad Amani[1,3] · Saeed Taghizadeh[2]

Received: 6 February 2018 / Accepted: 3 April 2018 / Published online: 9 April 2018

Abstract
Green synthetic method is an important process that can be used for the synthesis of iron nanoparticles in the field of nanotechnology because of its characteristics of low cost and high efficiency for industrial large-scale production. In this study, iron oxide nanoparticles (IONPs) were synthesized by a simple bio-reduction method. Aqueous leaf extract of *Daphne mezereum* was used as a reducing and stabilizing agent. Ultraviolet–visible (UV–vis) absorption spectroscopy was used to monitor the dye removing ability of IONPs. Also, IONPs were characterized by transmission electron microscopy (TEM), particle size analysis (PSA), Fourier transform infrared (FT-IR) spectroscopy, X-ray diffractometer (XRD), vibrating sample magnetometer (VSM), and thermo gravimetric analysis (TGA). The average diameter of the prepared NPs ranged from 6.5 to 14.9 nm with a mean particle size of 9.2 nm. In addition, the synthesized iron nanoparticles were tested for dye removing activities. The decoloration efficiency of INPs catalyzed reaction was about 81% after 6 h. Thus, it could be concluded that *D. mezereum* aqueous leaf extract can be used efficiently in the production of iron oxide NPs for commercial applications in environmental fields.

1 Introduction

The dye wastewater emission is one of the important reasons of environmental pollution which is increasing extremely [1–4]. Also, water quality is potentially influenced by color as the first characteristic of wastewater [5]. A very small amount of dye in water can cause change in light penetration and thus decrease the photosynthesis of aquatic plants [6]. Many dyes such as azo dyes are toxic, mutagenic and carcinogenic, so aquatic organisms as well as humans are exposed to this serious hazard [7–10]. Dye removing is difficult due to their resistance to biological degradation [11]. Numerous traditional technologies, including photocatalytic degradation [12–14], adsorption on activated carbon [15, 16], bacterial action [17], and electrochemical degradation [18, 19] have been expanded to remove dyes from wastewater. Between various techniques, adsorption is an efficient method to remove dyes particularly when they are recoverable and non-biodegradable [20].

Nanomaterials are one of the greatest and applicable elements in today's research; nanomaterials can form different networks ranging from simple to complicated networks which are important to materials chemistry and the existence of life [21–24].

Nowadays, iron nanomaterials (INPs) due to their versatile properties and high catalytic activities and the higher intrinsic reactivity of its surface sites have received great attention from researchers in different fields such as food-related applications [25], medical uses [26], biosensing applications [27], degradation of environmental organic contaminants [28], catalysis [29], magnetic storage media [30], magnetic field-assisted separations [31] and analyses [32]. Iron oxide nanoparticles as dye removing materials are used for maintaining a healthy environment [33]. To produce nanostructured iron particles, many methods including

✉ Ali Mohammad Amani
Amani_a@sums.ac.ir

✉ Saeed Taghizadeh
staghizadeh@sums.ac.ir

[1] Department of Medical Nanotechnology, School of Advanced Medical Sciences and Technologies, Shiraz University of Medical Sciences, Shiraz, Iran

[2] Department of Medical Biotechnology, School of Advanced Medical Sciences and Technologies, Shiraz University of Medical Sciences, Shiraz, Iran

[3] Pharmaceutical Sciences Research Center, Shiraz University of Medical Sciences, Shiraz, Iran

template-assisted synthesis method [34], hydrothermal synthesis [35], vapor–solid growth techniques [36], sol–gel process [37], chemical co-precipitation [38], thermal decomposition [39] and ultraviolet radiation and aerosol [40], have been used in an enormous number of studies on development of synthetic methods. Ideally, the synthetic method should be able to eliminate toxicity and make the nanoparticles more biocompatible [41]. Beside all the above mentioned methods, iron oxide nanoparticles obtained from biological methods such as fast and easy plant-mediated synthesis and microorganism-based procedures, are also being investigated [42, 43]. Besides these properties, the time consumed and the obligatory constraint of aseptic conditions are limiting factors for microorganism-based procedures. The plant-mediated synthesis of iron nanoparticles is more applicable than the other biological methods by the way of eliminating cumbersome process such as maintaining the cell culture [44–46]. Extraction and separation can be easily scaled up for the large-scale synthesis of nanoparticles, so in the recent years, iron oxide nanoparticles have been synthesized using various plant-mediated procedures [33]. Green-synthesized INPs has been recently examined for dye degradation and because of the easy availability of plants in nature, it makes them more applicable [47].

In this paper, the iron oxide NPs were synthesized using *Daphne mezereum* aqueous leaf extract and the prepared NPs were characterized using TEM, PSA, XRD, FT-IR, TGA, and VSM analysis. The present paper conducted to assess the dye removing potential of green-synthesized iron NPs with Ultraviolet–visible (UV–vis) absorption spectroscopy assay.

2 Materials and methods

2.1 Chemicals

Dried leaves of *D. mezereum* were purchased from a local shop (Shiraz, Fars, Iran). Ferric chloride hexa hydrate ($FeCl_3{\cdot}6H_2O$) was purchased from Merck chemicals (CAS #: 10025-77-1). Prepared solutions of ferric chloride were stored in aluminum foil wrapped polypropylene tube at refrigerator temperature. All glasswares were washed with concentrated HCL and deionized water before any use. Ultrapure deionised H_2O (Milli-Q, Millipore, Millipore Co., Bedford, MA, USA) was used for all synthesis reactions and leaf extract preparations.

2.2 Leaf extract preparation

To remove any mud and dust, dried leaves were washed with deionized water and dried at room temperature. Using about a 5% (w/v) mixture of dried leaves in deionized water has been the most common ratio for leaf extract preparation in previous experiments [41]. Consequently, 5 g dried leaves were boiled in 100 ml deionized water for 15 min using a heater mantel under reflux. The mixture was cooled to room temperature and filtered through a Whatman filter paper (Reeve angel, Grade 201). The prepared extract was centrifuged at 2000 rpm for 5 min to remove leaf microparticles. The resulting clear solution was sealed in polypropylene tubes and refrigerated.

2.3 Synthesis of INPs

Synthesis of INPs was conducted using a 10 ml reaction liquid. In practice, 1 ml iron precursor ($FeCl_3{\cdot}6H_2O$, 0.1 M) was added to 9 ml leaf extract while stirring vigorously at room temperature. After 24 h, the reaction mixture was centrifuged and the resulting black pellet was washed with deionized water and dried in an oven at 50 °C.

2.4 Characterization of INPs

The visual appearance and morphology of prepared INPs were evaluated by transmission electron microscopy (TEM). A drop of well-dispersed nanoparticles was placed on a carbon-coated copper grid and then dried at room temperature. The TEM micrographs were taken on a Philips CM 10, TEM, operated at high voltage (HT) 100 kV. Particle size analyses were conducted using ImageJ software version 1.47v. The hydrodynamic diameters of particles were measured using a Microtrac S3500 particle size analyzer. FT-IR spectra were obtained with KBr pellets in the range 400–4000 cm^{-1}. Prepared INPs were mixed and pressed with 150 mg KBr and the spectra were taken using a on a Bruker, Vertex 70, FT-IR spectrometer. The XRD measurements were carried out using a Siemens D5000 X-ray diffractometer. The crystallinity and composition of the INPs were analyzed over a 2θ range from 20° to 90° at a scan rate of 2° min^{-1} [48, 49]. Thermo gravimetric analysis (TGA) was performed by heating at a constant rate of 10 °C/min from 50 to 600 °C under argon atmosphere. The magnetic measurements were evaluated using a vibration sample magnetometer (VSM) at room temperature with increasing magnetic field up to 10 kOe and field sweeping from − 10 to + 10 kOe at Meghnatis Daghigh Kavir Co.

2.5 Removing of methyl orange (MO)

For degradation of methyl orange dye, all processes were carried out under atmospheric pressure and in single-use 10 ml reaction volume, by stirring magnetically at 150 rpm. In the typical experiment, 10 mg of synthesized nanoparticles were added to solutions containing 8 ml methyl orange (25 mg/l) and 1 ml H_2O_2 (10%). The concentrations of MO

after different times of contact (15, 30, 60, 120, 180, 240, 300, and 360 min) were determined with a Hitachi U-0080D UV–vis spectrophotometer (Tokyo Japan) at λ max = 465 nm and calibration curve was obtained using the standard MO solution. Also, to evaluate the ability of hydrogen peroxide alone in the decomposition of methyl orange, a blank sample was tested without nanoparticles. All experiments were performed in triplicate.

3 Results and discussion

3.1 Characterization of INPs

After addition of 0.1 M iron solution (III) to the *D. mezereum* leaf extract, the color of the mixture changes from yellow to intense brown, indicating the formation of iron-containing nanoparticles.

TEM micrograph and PSA data of the INPs synthesized by *D. mezereum* extract are shown in Fig. 1. The particle size distribution of biosynthesized INPs was in the range of 6.5–14.9 nm with a mean particle size of 9.2 nm. TEM showed that the majority of INPs were spherical in shape with only a limited degree of aggregation. It was observed that these nanoparticles were surrounded by a thin layer of biological matrix showing the role of biological compounds in *D. mezereum* extract for reducing the Fe (III) ions to INPs.

The FT-IR spectrum of synthesized INPs is shown in Fig. 2. The FT-IR spectroscopic data were carried to characterize the functional groups of biomolecules in *D. mezereum* extract that was involved in reduction and stabilization of the INPs. The adsorption bands around 516 cm^{-1} corresponded to Fe-O stretches of Fe_2O_3 or Fe_3O_4. Furthermore,

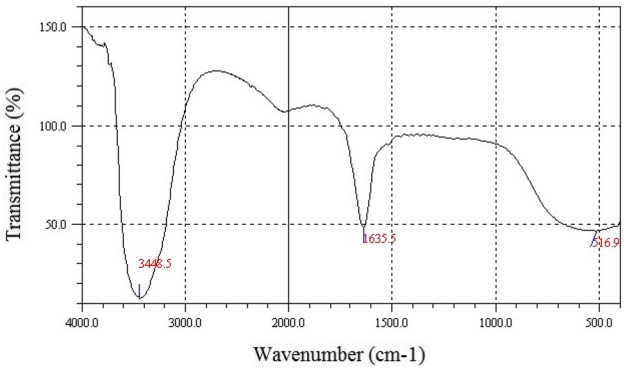

Fig. 2 The FT-IR spectra of synthesized INPs

the peaks at 3448 and 1635 cm^{-1} refer to the O–H of H bond or carboxylic acid and C=C ring stretching on the synthesized INPs surface. The functional groups introduced in the nanoparticle production process indicated that biochemical compounds from *D. mezereum* extract decorated the surface of biosynthesized nanoparticles and enhance the interactions with water molecules that results in more stable colloids.

The XRD pattern of the INPs produced by *D. mezereum* extract is shown in Fig. 3. The XRD pattern of INPs showed deficiency in distinctive diffraction peaks which corresponded to amorphous nature of these nanoscale particles. The broad peak in region about $2\theta = 25$ represents the organic biomolecules covering the surface of the nanoparticles [48, 49].

Figure 4 shows the magnetic characteristics of synthesized INPs evaluated by a vibrating sample magnetometer at room temperature. A linear MH graph with no hysteresis loop was observed, which indicates that the produced

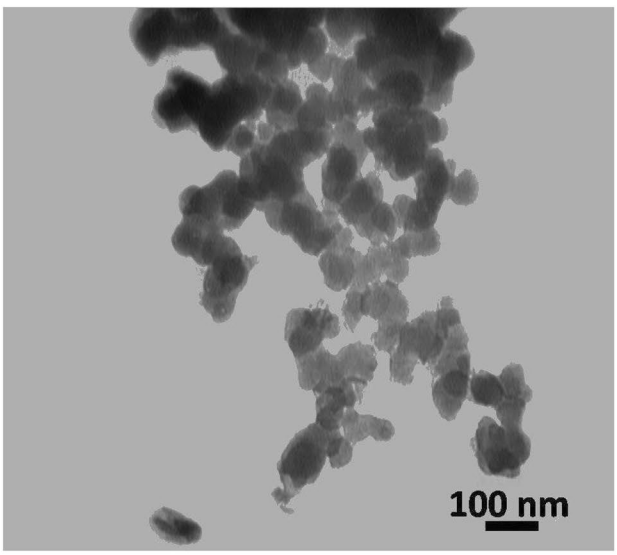

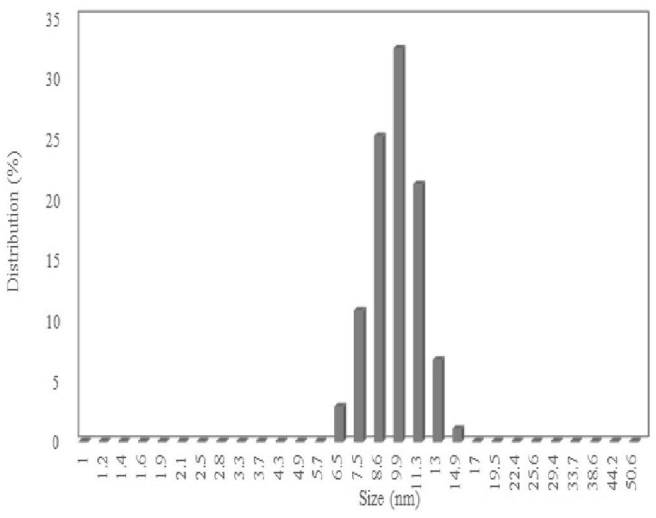

Fig. 1 TEM micrograph and particle size distribution diagram of the INPs

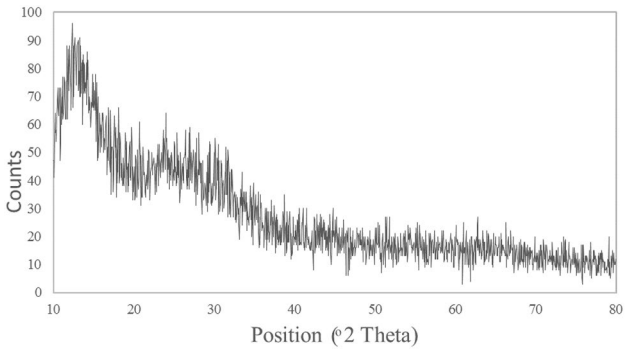

Fig. 3 XRD pattern of the green-synthesized INPs

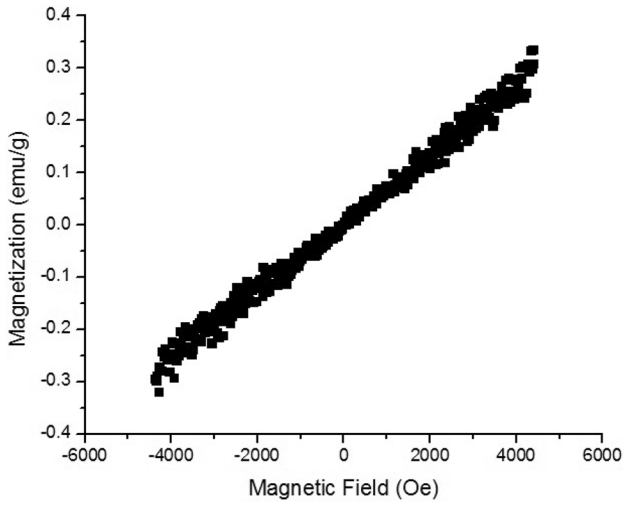

Fig. 4 Magnetization curve of biosynthesized INPs

nanoparticles have paramagnetic properties. Paramagnetism refers to a property of materials in which they are weakly attracted by a strong externally applied magnetic field, and form internal induced magnetic fields in the direction of the applied magnetic field.

TGA curve of biosynthesized INPs for measuring the purity and composition of the sample is provided in Fig. 5. The NPs mass starts to fluctuate around 100% at below 200 °C, which is attributed to residual and adsorbed water with the INPs [50]. The results show that after gradually reducing the weight of nanoparticles at low temperatures, a sudden drop in weight occurs up to 200 °C. Previous research results show that at temperatures below 200 °C, biomolecule compounds covering nanoparticles have a thermal stability. However, these biomaterials begin to decompose and degrade at high temperatures [41, 51].

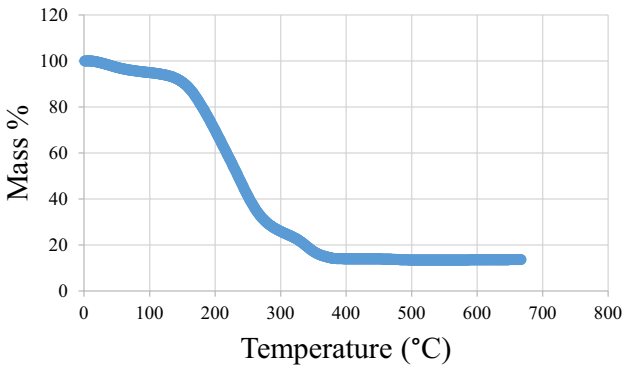

Fig. 5 TGA curve of INPs

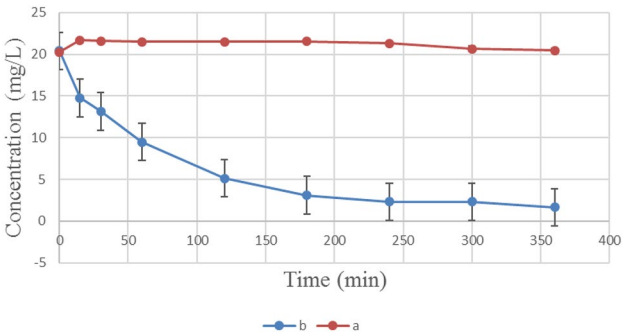

Fig. 6 Dye removal diagram using H_2O_2 alone (**a**) and H_2O_2 with iron nanoparticles (**b**)

3.2 Dye removing assay

The MO decolorization kinetic by the synthesized INPs is presented in Fig. 6. As indicated in this figure, in sample with absence of INPs, no significant decolouration activity was observed after 6 h. However, the results shows that the reduction of MO with H_2O_2 in the presence of catalytic activity of prepared NPs occurs at a very fast rate in initial reaction time and the efficiency of decolorization decreased after a reaction of 180 min with the NPs. The decoloration efficiency of INPs catalyzed reaction was about 81% after 6 h. These results indicated that by employing green-synthesized INPs by *D. mezereum* extract, MO azo dye can be oxidated by a Fenton-like reaction which is a combination of Fe^{2+} and hydrogen peroxide according to the following formula (I and II). The –N=N– double bond in MO azo dye is the chromophoric group and cleavage of this bond by $OH^{\bullet}$ leads to MO decolorization [52, 53]. It is known that Fe nanoparticles green synthesized by different leaf extracts have different capabilities for the removal of methyl orange dye in liquid environments. For instance, Muthukumar and Manickam investigated the decolourization of MO using both FeO nanoparticles green synthesized by *Amaranthus*

spinosus leaf extract and chemically synthesized by NaBH4. 750 ml of 100 ppm MO dye solution was treated with 250 mg/l of NPs under the average sunlight irradiation of 1000 W/m^2 at 38 ± 2 °C for 6 h. The percentage decolourization of methyl orange was 75% for green-synthesized iron oxide nanoparticles. Whereas, the decolourization potential of FeO nanoparticles chemically synthesized by $NaBH_4$ was even lower than these particles [54]. Also, Ebrahiminezhad et al. have reported that iron nanoparticles synthesized by aqueous extract of Mediterranean cypress could be a more effective material for catalytic MO dye degradation with 95.8% removal efficiency only after 6 h [55].

$$Fe^{2+} + H_2O_2 \rightarrow Fe3^{+} + OH^{\bullet} + OH^{-} \quad (1)$$

$$Fe^{3+} + H_2O_2 \rightarrow Fe^{2+} + OOH^{\bullet} + H^{+} \quad (2)$$

4 Conclusion

In summary, an eco-friendly synthesis process has been successfully employed for synthesis of iron oxide NPs using *D. mezereum* aqueous leaf extract with no additional agents. The organic compound of *D. mezereum* leaf extract had a significant impact on the stability of nanoparticles. The results of this study showed that synthesized IONPs were more effective catalyst to degrade MO dye, so that 75% of total dye with 20 mg per liter initial concentration was removed after only 6 h in the solution containing 10 mg the IONPs with H_2O_2. Overall, these results suggest that green synthesis of iron oxide nanoparticles has potential as an effective, economical and useful process for many scientific and technical applications in future, including treatment of toxic organic contamination in the environment.

Acknowledgements This work was financially supported by School of Advanced Medical Sciences and Technologies, Shiraz University of Medical Sciences, Shiraz, Iran.

References

1. V.K. Gupta, R. Jain, A. Nayak, S. Agarwal, M. Shrivastava, Removal of the hazardous dye—tartrazine by photodegradation on titanium dioxide surface. Mater. Sci. Eng. C **31**(5), 1062–1067 (2011)
2. D.I. Rinawati, D.P. Sari, B. Purwanggono, A.T. Hermawan, *Environmental Impact Analysis of Batik Natural Dyes Using Life Cycle Assessment*. In: AIP conference proceedings, AIP Publishing, Melville, NY, p 020044 (2017)
3. M. Mokhtar, Application of synthetic layered sodium silicate magadiite nanosheets for environmental remediation of methylene blue dye in water. Materials **10**, 760 (2017)
4. L.E. Cuervo, M.F. Gomes, C.V. Da Silva, A.M. de Freitas, E. Tiburtius, Degradation and ecotoxicity of dye Reactive Black 5 after reductive-oxidative process. Environ Sci Pollut Res Int 24(7), 6126–6134 (2017)
5. J. Breneman, H. Blasinski, J.E. Farrell, *The Color of Water: Using Underwater Photography to Estimatewater Quality*. In: Digital Photography, p. 90230R (2014)
6. Z.-M. Ni, S.-J. Xia, L.-G. Wang, F.-F. Xing, G.-X. Pan, Treatment of methyl orange by calcined layered double hydroxides in aqueous solution: adsorption property and kinetic studies. J. Colloid Interface Sci. **316**(2), 284–291 (2007)
7. F.M.D. Chequer, T.M. Lizier, R. de Felício, M.V.B. Zanoni, H.M. Debonsi, N.P. Lopes, D.P. de Oliveira, The azo dye Disperse Red 13 and its oxidation and reduction products showed mutagenic potential. Toxicol. In Vitro **29**(7), 1906–1915 (2015)
8. B.J. Brüschweiler, C. Merlot, Azo dyes in clothing textiles can be cleaved into a series of mutagenic aromatic amines which are not regulated yet. Regul. Toxicol. Pharmacol. **88**, 214–226 (2017)
9. T.N.J.I. Edison, R. Atchudan, M.G. Sethuraman, Y.R. Lee, Reductive-degradation of carcinogenic azo dyes using *Anacardium occidentale* testa derived silver nanoparticles. J. Photochem. Photobiol. B **162**, 604–610 (2016)
10. V. Martínek, M. Stiborová, Metabolism of carcinogenic azo dye Sudan I by rat, rabbit, minipig and human hepatic microsomes. Collect. Czechoslov. Chem. Commun. **67**(12), 1883–1898 (2002)
11. K. Lokesh, R. Sivakiran, Biological methods of dye removal from textile effluents—a review. J. Biochem. Technol. **3**(5), 177–180 (2014)
12. X. Chen, Z. Wu, D. Liu, Z. Gao, Preparation of ZnO photocatalyst for the efficient and rapid photocatalytic degradation of azo dyes. Nanos. Res. Lett. 12(1), 143 (2017)
13. G. Lucena, L. de Lima, L. Honório, A. de Oliveira, R. Tranquilim, E. Longo, A. de Souza, A.d..S. Maia, I. dos Santos, CaSnO 3 obtained by modified Pechini method applied in the photocatalytic degradation of an azo dye. Cerâmica **63**(368), 536–541 (2017)
14. E. Kusmierek, P. Mierczynski, A. Kedziora, M. Nowosielska, W. Maniukiewicz, S. Vorobyov, R. Vitkovskaya, T.P. Maniecki, Photocatalytic degradation of an azo dye over novel monometallic copper catalysts supported on fibreglass. Catal. Lett. **147**(9), 2448–2461 (2017)
15. G.M.D. Ferreira, G.M.D. Ferreira, M.C. Hespanhol, J. de Paula Rezende, A.C. dos Santos Pires, L.V.A. Gurgel, L.H.M. da Silva, Adsorption of red azo dyes on multi-walled carbon nanotubes and activated carbon: a thermodynamic study. Colloids Surf. A **529**, 531–540 (2017)
16. E. Ghasemian, Z. Palizban, Comparisons of azo dye adsorptions onto activated carbon and silicon carbide nanoparticles loaded on activated carbon. Int. J. Environ. Sci. Technol. **13**(2), 501–512 (2016)
17. R. Khan, U.C. Banerjee, Decolorization of Azo Dyes by Immobilized Bacteria. *Biodegradation of Azo Dyes* (Springer, Berlin, 2010), pp. 73–84
18. Z.M. Redha, H.A. Yusuf, H.A. Ahmed, P.R. Fielden, N.J. Goddard, S.J. Baldock, A miniaturized injection-moulded flow-cell with integrated conducting polymer electrodes for on-line electrochemical degradation of azo dye solutions. Microelectron. Eng. **169**, 16–23 (2017)
19. Z.U.H. Khan, A. Khan, Y. Chen, A. ullah Khan, N.S. Shah, N. Muhammad, B. Murtaza, K. Tahir, F.U. Khan, P. Wan, Photo catalytic applications of gold nanoparticles synthesized by green route and electrochemical degradation of phenolic azo dyes using AuNPs/GC as modified paste electrode. J. Alloy. Compd. **725**, 869–876 (2017)
20. M. Iram, C. Guo, Y. Guan, A. Ishfaq, H. Liu, Adsorption and magnetic removal of neutral red dye from aqueous solution using Fe_3O_4 hollow nanospheres. J. Hazard. Mater. **181**(1), 1039–1050 (2010)

21. B. Maddah, A simple colorimetric kit for determination of ketamine hydrochloride in water samples. Anal. Methods **7**(24), 10364–10370 (2015)
22. A. Ebrahiminezhad, S. Taghizadeh, A. Berenjian, A. Rahi, Y. Ghasemi, Synthesis and characterization of silver nanoparticles with natural carbohydrate capping using *Zataria multiflora*. Adv. Mater. Lett. **7**(11), 939–944 (2016)
23. A. Ebrahiminezhad, S. Taghizadeh, Y. Ghasemi, Green synthesis of silver nanoparticles using Mediterranean Cypress (*Cupressus sempervirens*) leaf extract. Am. J. Biochem. Biotechnol. **13**(1), 1–6 (2017)
24. A. Ebrahiminezhad, S. Taghizadeh, A. Berenjian, F. Heidaryan Naeini, Y. Ghasemi, Green synthesis of silver nanoparticles capped with natural carbohydrates using ephedra intermedia. Nanosci Nanotechnol Asia **7**(1), 104–112 (2017)
25. M. Cao, Z. Li, J. Wang, W. Ge, T. Yue, R. Li, V.L. Colvin, W.Y. William, Food related applications of magnetic iron oxide nanoparticles: enzyme immobilization, protein purification, and food analysis. Trends Food Sci. Technol. **27**(1), 47–56 (2012)
26. A.K.A. Silva, A. Espinosa, J. Kolosnjaj-Tabi, C. Wilhelm, F. Gazeau, Medical applications of iron oxide nanoparticles. Iron Oxides Nat. Appl., 425–472 (2016)
27. M. Hasanzadeh, N. Shadjou, M. de la Guardia, Iron and iron-oxide magnetic nanoparticles as signal-amplification elements in electrochemical biosensing. TrAC Trends Anal. Chem. **72**, 1–9 (2015)
28. Y. Wang, H. Zhao, G. Zhao, Iron-copper bimetallic nanoparticles embedded within ordered mesoporous carbon as effective and stable heterogeneous Fenton catalyst for the degradation of organic contaminants. Appl. Catal. B **164**, 396–406 (2015)
29. J.M. Walker, J.M. Zaleski, A simple route to diverse noble metal-decorated iron oxide nanoparticles for catalysis. Nanoscale **8**(3), 1535–1544 (2016)
30. W.J. Yu, C. Liu, L. Zhang, P.X. Hou, F. Li, B. Zhang, H.M. Cheng, Synthesis and electrochemical lithium storage behavior of carbon nanotubes filled with iron sulfide nanoparticles. Adv. Sci. **3**, (10) (2016)
31. A. Massoud, H. Mahmoud, Evaluation of hybrid polymeric resin containing nanoparticles of iron oxide for selective separation of In (III) from Ga (III). J. Inorg. Organomet. Polym Mater. **27**(6), 1806–1815 (2017)
32. Y. Bentahir, S. Elmarhoum, R. Salghi, M. Algarra, A. Ríos, M. Zougagh, Dispersed synthesis of uniform Fe_3O_4 magnetic nanoparticles via in situ decomposition of iron precursor along cotton fibre for Sudan dyes analysis in food samples. Food Addit. Contam. Part A **34**(11), 1853–1862 (2017)
33. A. Ebrahiminezhad, A. Zare-Hoseinabadi, A.K. Sarmah, S. Taghizadeh, Y. Ghasemi, A. Berenjian, Plant-mediated synthesis and applications of iron nanoparticles. Mol. Biotechnol. **60**(2), 1–15 (2017)
34. D. Mishra, H. Zabel, S. Ulyanov, V. Romanov, V. Uzdin, Template assisted self-assembly of iron oxide nanoparticles: an X-ray structural analysis. J. Appl. Phys. **115**(5), 054104 (2014)
35. B. Palagiri, R. Chintaparty, R.R. Nagireddy, V.S.R. Imma Reddy, Influence of synthesis conditions on structural, optical and magnetic properties of iron oxide nanoparticles prepared by hydrothermal method. Phase Transit. **90**(6), 578–589 (2017)
36. S. Futko, B. Shulitskii, V. Labunov, E. Ermolaeva, Simulation of the kinetics of growth of iron nanoparticles in the process of chemical vapor deposition of hydrocarbons with injection of ferrocene for the synthesis of carbon-nanotube arrays. J. Eng. Phys. Thermophys. **88**(6), 1432–1441 (2015)
37. Z.N. Kayani, S. Arshad, S. Riaz, S. Naseem, Synthesis of iron oxide nanoparticles by sol–gel technique and their characterization. IEEE Trans. Magn. **50**(8), 1–4 (2014)
38. A. Taufiq, S. Pratapa, M. Zainuri, Various magnetic properties of magnetite nanoparticles synthesized from iron-sands by coprecipitation method at room temperature, Mater. Sci. Forum **827**, 229 (2015)
39. N.J. Orsini, B. Babić-Stojić, V. Spasojević, M. Calatayud, N. Cvjetićanin, G. Goya, Magnetic and power absorption measurements on iron oxide nanoparticles synthesized by thermal decomposition of Fe (acac) 3. J. Magn. Magn. Mater. **449**, 286–296 (2018)
40. G. Kastrinaki, S. Lorentzou, G. Karagiannakis, M. Rattenbury, J. Woodhead, A. Konstandopoulos, Parametric synthesis study of iron based nanoparticles via aerosol spray pyrolysis route. J. Aerosol Sci. **115**, 96–107 (2018)
41. A. Ebrahiminezhad, A. Zare-Hoseinabadi, A. Berenjian, Y. Ghasemi, Green synthesis and characterization of zero-valent iron nanoparticles using stinging nettle (*Urtica dioica*) leaf extract. Green Process. Synth. **6**, 469–475 (2017)
42. A. Ebrahiminezhad, M. Zare, S. Kiyanpour, A. Berenjian, S.V. Niknezhad, Y. Ghasemi, Biosynthesis of xanthan gum coated iron nanoparticles by using *Xanthomonas campestris*. IET Nanobiotechnol. **12**, 254–258 (2017)
43. M. Seifan, A. Ebrahiminezhad, Y. Ghasemi, A.K. Samani, A. Berenjian, Amine-modified magnetic iron oxide nanoparticle as a promising carrier for application in bio self-healing concrete. Appl. Microbiol. Biotechnol. **102**, 1–10 (2017)
44. R. Dinali, A. Ebrahiminezhad, M. Manley-Harris, Y. Ghasemi, A. Berenjian, Iron oxide nanoparticles in modern microbiology and biotechnology. Crit. Rev. Microbiol. **43**(4), 493–507 (2017)
45. S. Kianpour, A. Ebrahiminezhad, M. Mohkam, A.M. Tamaddon, A. Dehshahri, R. Heidari, Y. Ghasemi, Physicochemical and biological characteristics of the nanostructured polysaccharide-iron hydrogel produced by microorganism *Klebsiella oxytoca*. J. Basic Microbiol. 57(2), 132–140 (2017)
46. Y.L. Raĭkher, V. Stepanov, S. Stolyar, V. Ladygina, D. Balaev, L. Ishchenko, M. Balasoiu, Magnetic properties of biomineral particles produced by bacteria *Klebsiella oxytoca*. Phys. Solid State **52**(2), 298–305 (2010)
47. S. Saif, A. Tahir, Y. Chen, Green synthesis of iron nanoparticles and their environmental applications and implications. Nanomaterials **6**(11), 209 (2016)
48. E.C. Njagi, H. Huang, L. Stafford, H. Genuino, H.M. Galindo, J.B. Collins, G.E. Hoag, S.L. Suib, Biosynthesis of iron and silver nanoparticles at room temperature using aqueous sorghum bran extracts. Langmuir **27**(1), 264–271 (2010)
49. Z. Xiao, M. Yuan, B. Yang, Z. Liu, J. Huang, D. Sun, Plant-mediated synthesis of highly active iron nanoparticles for Cr (VI) removal: Investigation of the leading biomolecules. Chemosphere **150**, 357–364 (2016)
50. B.S. Inbaraj, T.-Y. Tsai, B.-H. Chen, Synthesis, characterization and antibacterial activity of superparamagnetic nanoparticles modified with glycol chitosan. Sci. Technol. Adv. Mater. **13**(1), 015002 (2012)
51. Z. Durmus, H. Kavas, M.S. Toprak, A. Baykal, T.G. Altınçekiç, A. Aslan, A. Bozkurt, S. Coşgun, L-lysine coated iron oxide nanoparticles: synthesis, structural and conductivity characterization. J. Alloy. Compd. **484**(1), 371–376 (2009)
52. T. Shahwan, S.A. Sirriah, M. Nairat, E. Boyacı, A.E. Eroğlu, T.B. Scott, K.R. Hallam, Green synthesis of iron nanoparticles and their application as a Fenton-like catalyst for the degradation of aqueous cationic and anionic dyes. Chem. Eng. J. **172**(1), 258–266 (2011)
53. Z. Wang, C. Fang, M. Megharaj, Characterization of iron–polyphenol nanoparticles synthesized by three plant extracts and their fenton oxidation of azo dye. ACS Sustain. Chem. Eng. **2**(4), 1022–1025 (2014)
54. H. Muthukumar, M. Matheswaran, Amaranthus spinosus leaf extract mediated FeO nanoparticles: physicochemical traits, photocatalytic and antioxidant activity. ACS Sustain. Chem. Eng. **3**(12), 3149–3156 (2015)

55. A. Ebrahiminezhad, S. Taghizadeh, Y. Ghasemi, A. Berenjian, Green synthesized nanoclusters of ultra-small zero valent iron nanoparticles as a novel dye removing material. Sci. Total Environ. **621**, 1527–1532 (2017)